

Superconducting properties of strongly underdoped $\text{Bi}_2\text{Sr}_2\text{CaCu}_2\text{O}_{8+x}$ single crystalsM. Li,¹ C. J. van der Beek,² M. Konczykowski,² A. A. Menovsky,³ and P. H. Kes¹¹*Kamerlingh Onnes Laboratory, Leiden University, P.O. Box 9504, 2300 RA Leiden, The Netherlands*²*Laboratoire des Solides Irradiés, Ecole Polytechnique, 91128 Palaiseau, France*³*Van der Waals-Zeeman Laboratorium, Universiteit van Amsterdam, Valckenierstraat 65, 1018 XE Amsterdam, The Netherlands*

(Received 6 September 2001; revised manuscript received 10 December 2001; published 24 June 2002)

We have successfully obtained high-quality strongly underdoped $\text{Bi}_2\text{Sr}_2\text{CaCu}_2\text{O}_{8+x}$ (Bi-2212) single crystals by growth in reduced oxygen partial pressure. Doping levels could subsequently be varied from underdoped through optimally doped to overdoped by a straightforward post-annealing treatment. We have characterized the obtained crystals by low-field magnetic screening experiments as well as by reversible magnetization in fields to several tesla and report the values of the penetration depth and carrier density.

DOI: 10.1103/PhysRevB.66.024502

PACS number(s): 74.72.Hs, 74.62.Dh, 74.40.+k

I. INTRODUCTION

Underdoped high- T_c superconductors (HTS's) are interesting because they show the universal pseudogap formation in addition to the superconducting gap. They are also interesting from the point of view of vortex physics because of their strong anisotropy and layered nature. The doping level of the $\text{Bi}_2\text{Sr}_2\text{CaCu}_2\text{O}_{8+x}$ (Bi-2212) compound can be varied either by partial cation replacement or by oxygen doping. For instance, to get underdoped samples, Sr or Ca can be partially substituted by cations of higher valencies, such as Y,¹ or Cu can be partially replaced by Zn or Ni.² To get more overdoped levels Bi has been partially replaced by Pb.³ However, substitution techniques usually lead to inhomogeneous crystals exhibiting strong irreversibility which hinders the study of superconducting properties. It is also rather difficult to distinguish the effect of substitution from that of various atomic displacements which may occur. The disorder due to the displacements together with d -wave symmetry leads to a reduction of T_c which should be distinguished from the effect of the change in carrier concentration.⁴ In order to avoid disordering, one often chooses to control the oxygen concentration by means of post-anneal treatments in a gas atmosphere with different partial pressures of oxygen. The post-anneal procedures work well to obtain optimally doped and overdoped crystals since the as-grown Bi-2212 crystals in air are already overdoped.⁵ To extend the post-anneal treatment of Bi-2212 in order to obtain strongly underdoped samples one needs an extreme reduction of oxygen partial pressure which easily leads to a decomposition of the single crystals.⁶ In addition, even the most careful post-anneal treatments gave rise to underdoped crystals with relatively broad resistive transitions ($\delta T_c \approx 6-10$ K).^{7,8} Therefore we tried to find a way for preparing Bi-2212 crystals which are uniform and underdoped as-grown.

In this paper we present a convenient way to obtain such strongly underdoped single crystals of Bi-2212. We use the traveling solvent floating zone (TSFZ) technique at relatively *low partial pressures of oxygen* and successfully obtained high-quality crystals with T_c as low as 65 K and with sharp superconducting transitions $\delta T_c \leq 2.5$ K. We studied the influence of post-anneal treatments at different oxygen pressures on the superconducting properties by measuring the

reversible magnetization. The small bulk pinning gives access to a wide field and temperature range; also, geometrical and surface effects are negligible over an extended region of the phase diagram. We have analyzed the reversible magnetization of the strongly underdoped samples using existing theoretical models and we find that the effect of thermal fluctuations is much smaller than predicted for entirely decoupled pancake vortices, indicating that the fluctuating objects are stacks of small numbers of pancakes and that near T_c short-range phase coherence extends over small distances ($\geq 3s$) even in fields of a few tesla (s is the layer spacing). Accounting for the influence of this effect, the modified term $dM/d(\ln H) \sim \lambda^2(0)/\lambda^2(T)$ versus T could be fitted both by the d -wave pairing model⁹ and the clean-limit BCS theory.¹⁰ By using two-dimensional (2D) scaling theory,¹¹ the Ginzburg-Landau (GL) coherence length ξ could be determined as well.

II. EXPERIMENTS

$\text{Bi}_2\text{Sr}_2\text{CaCu}_2\text{O}_{8+x}$ single crystals were grown by the TSFZ method.^{5,12} Several growth runs were carried out under different partial pressures of oxygen P_{O_2} by mixing oxygen with pure argon. We choose P_{O_2} 's of 10 mbar, 25 mbar, 100 mbar, 130 mbar, and 200 mbar. Hereafter we denoted samples produced from these runs by Bi-10 to Bi-200, respectively.

The chemical composition, homogeneity, and quality of the as-grown Bi-2212 single crystals were checked by electron probe microanalysis (EPMA), x-ray diffraction, and magneto-optically imaging the penetration of magnetic flux into the superconducting phase.¹³ Magnetization measurements were carried out in a superconducting quantum interference device (SQUID) magnetometer with the field applied parallel to the c axis and a 4 cm scan length. For the Bi-25 samples we determined the contribution from the sample holder by measuring between 100 K and 240 K. This background signal turned out to be temperature independent; therefore, all the presented magnetization data were obtained by subtracting the background signal measured at 120 K. The superconducting transition temperature T_c was determined from ac susceptibility measurements in an ac field of 1 G

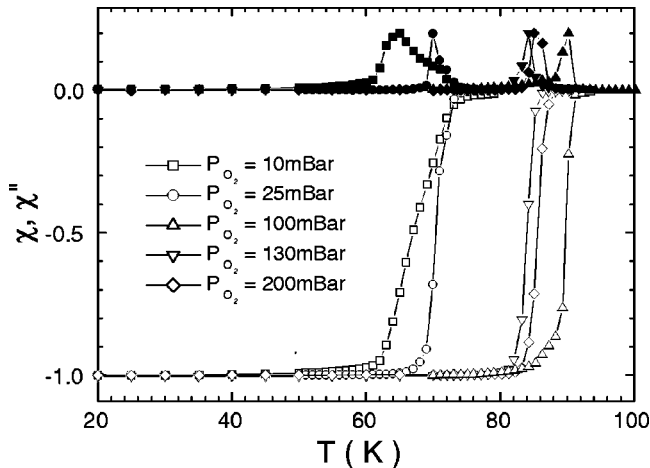


FIG. 1. Magnetic ac susceptibility [$\chi'(T)$ and $\chi''(T)$] of the as-grown samples, from Bi-10 to Bi-200, measured with ac field $h_{ac}=1$ G and frequency = 171 Hz.

parallel to the c axis and with a frequency of 171 Hz. The remanent dc field of the superconducting coil was eliminated by degaussing the magnet. The linear extrapolation of the $\chi'(T)$ data to zero defined T_c . The width of the transition δT_c was taken as the temperature difference between 10% and 90% of the full ac field expulsion.

Our reversible magnetization experiments were mainly carried out on three single crystals cleaved from the same Bi-25 batch. Various doping levels were achieved by different post-anneal treatments performed for three days: (i) at 750 °C in air to obtain a nearly optimally doped crystal (this sample was denoted as Bi-25-OP, and its dimension was $2.36 \times 0.90 \times 0.017$ mm³), (ii) in flowing N₂ at 700 °C for the underdoped crystal (Bi-25-UD with dimensions $1.54 \times 0.73 \times 0.090$ mm³), and (iii) in flowing O₂ at 400 °C for the overdoped crystal (Bi-25-OV with dimensions $2.20 \times 0.53 \times 0.054$ mm³).

III. RESULTS AND DISCUSSIONS

A. Crystals properties

Figure 1 shows the temperature dependence of the ac susceptibility (χ' and χ'') of the different as-grown Bi-2212 single crystals extracted from the five as-grown rods, Bi-10 to Bi-200. Their chemical composition, c axis, T_c , and δT_c values are given in Table I. Figure 2 shows the T_c values of these samples plotted versus P_{O_2} . It is seen that T_c strongly

TABLE I. Characteristics of Bi-2212 single crystals grown in different partial oxygen pressures.

Crystal samples	Bi: Sr: Ca: Cu	c (nm)	T_c (K)	δT_c (K)
Bi-200	2.25:1.89:1.00:2	3.078	86.5	2.5
Bi-130	2.29:1.87:1.01:2	3.088	85.5	2.7
Bi-100	2.24:1.92:0.95:2	3.093	90.5	2.5
Bi-25	2.23:1.90:0.96:2	3.089	73.5	3.0
Bi-10	2.23:1.91:0.93:2	3.089	73	9.0

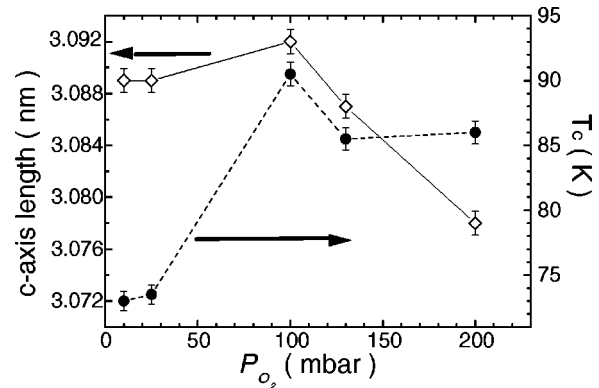


FIG. 2. T_c (●) and c -axis parameter (◇) vs the partial oxygen pressure P_{O_2} of as-grown samples from Bi-10 to Bi-200. The solid and dashed lines are guides to the eyes.

depends on the oxygen partial pressure during growth, while T_c of Bi-100 is as large as 90.5 K with a sharp transition ($\delta T_c \leq 2.5$ K) indicating a nearly optimally doped sample. Bi-10 and Bi-25 both have $T_c \sim 73$ K and are underdoped in oxygen. The much broader transition ($\delta T_c \sim 9$ K) and the greater difficulty to cleave sample Bi-10 indicate that its quality is inferior to that of the other crystals.

We also plot the length of the c axis in Fig. 2. According to high-pressure studies on Bi-2212,^{14,15} we would expect that the changes in T_c and the length of the c axis are proportional and given by $dT_c/d(\ln c) = 2.9 \times 10^3$ K. Comparing with the data we conclude that T_c of Bi-130 seems somewhat low, whereas T_c of Bi-200 is somewhat high. This unexpected nonsystematic behavior may be related to smaller Sr/Ca ratio in Bi-130 in comparison to that of Bi-200. For the overdoped Bi-2212 samples, experimental data showed that a slightly smaller Sr/Ca ratio yields a smaller T_c and vice versa.⁵ From Fig. 2 we also note that for the underdoped samples there is a strong decrease in T_c while the c -axis parameter remains almost constant. Since the cation concentrations of Bi-10, Bi-25, and Bi-100 are the same, the change in T_c has to come from the change of oxygen content.

Post-anneal treatments were carried out on samples from the batch Bi-25. The ac susceptibility of the post-annealed samples Bi-25-UD, Bi-25-OP, and Bi-25-OV together with the as-grown Bi-25 are shown in Fig. 3. We see that the doping levels change from strongly underdoped ($T_c = 65.0$ K) to nearly optimally doped ($T_c = 87.3$ K) and then to overdoped ($T_c = 77.0$ K). Notably, the superconducting transition of Bi-25-UD with $T_c = 65.0$ K is still sharp ($\delta T_c \leq 2.5$ K), almost the same as for the other doping levels. Usually the superconducting transitions for the underdoped HTSC samples were reported to be much broader than those of the optimally doped and overdoped states.^{4,16} We conclude that the doping levels of the as-grown, underdoped Bi-2212 crystals can be conveniently changed over a wide range.

The crystals from the Bi-25 batch appeared to be mostly free of line-shaped macrodefects, which are often reported to occur in as-grown-in-air Bi-2212 crystals. These line-shaped defects are believed to be intergrowths of the

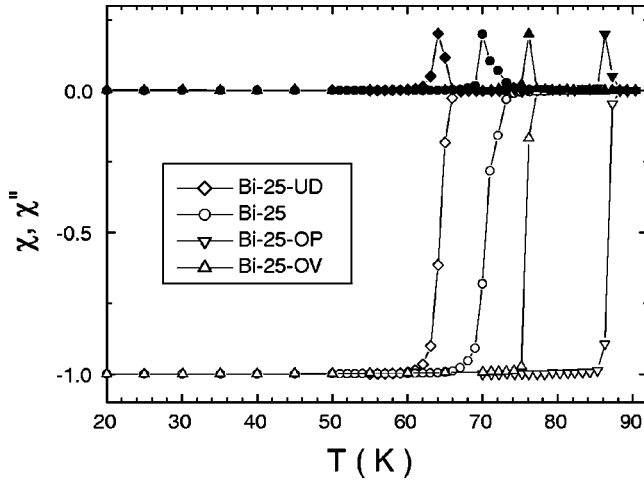


FIG. 3. Ac susceptibility [$\chi'(T)$ and $\chi''(T)$] of the samples Bi-25-UD (\diamond), Bi-25-OP (∇), and Bi-25-OV (\triangle) together with the as-grown Bi-25 (\circ).

$\text{Bi}_2\text{Sr}_2\text{Ca}_2\text{Cu}_3\text{O}_{10+x}$ (Bi-2223) phase.¹⁷ Such defects strongly affect vortex pinning and motion and give rise to very irregular flux line distributions.¹⁸ The presence of these extended, linear defects is easily seen in magneto-optical observations of magnetic flux penetration. A typical example is shown in Fig. 4(a) for a crystal from the Bi-200 batch in which linear defects were frequently observed. This phenomenon was mostly not observed on crystals from the Bi-25 batch. An example is shown in Fig. 4(b) where a regular “roof”-shaped pattern demonstrates the absence of extended defects. As a possible explanation, we note that during the growth in low oxygen partial pressures the heat input that controls the temperature at the solid-liquid interface was somewhat lower than when growing in air. It thus seems that the comparatively lower growing temperature suppresses the

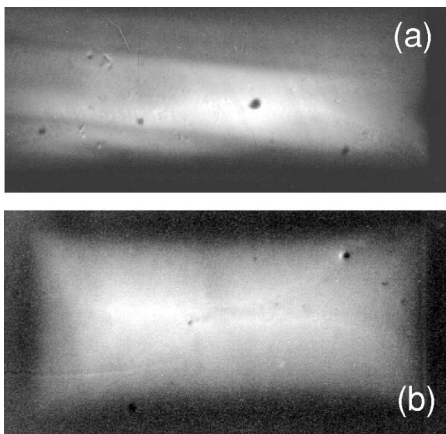


FIG. 4. Magneto-optic images of two Bi-2212 single crystals. (a) shows the image taken after removing a field of 483 G at 20 K for a crystal from the Bi-200 batch ($1.89 \times 0.69 \text{ mm}^2 \times 40 \text{ }\mu\text{m}$). The line-shaped defects are clearly visible. (b) shows an as-grown crystal from the Bi-25 batch (dimension $1.46 \times 0.67 \text{ mm}^2 \times 40 \text{ }\mu\text{m}$). The image was taken after the field was switched off from 475 G at 25 K.

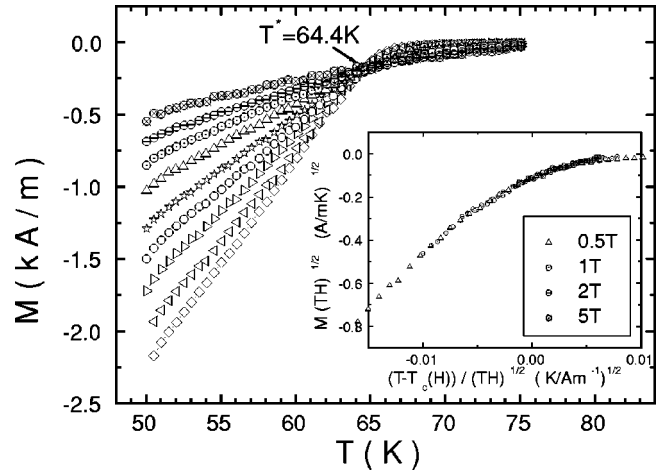


FIG. 5. The reversible magnetization of the sample Bi-25-UD as function of temperature in different magnetic fields: 0.01 T (\diamond), 0.02 T (\triangleleft), 0.05 T (\triangleright), 0.1 T (\circ), 0.2 T (\star), 0.5 T (\triangle), 1 T (\odot), 2 T (\ominus), and 5 T (\otimes). Inset: 2D scaling of the magnetization data of the same crystal for 0.5 T, 1 T, 2 T, and 5 T, respectively, with $H'_{c2} = 0.82 \text{ T/K}$ and $T_c(0) = 69.6 \text{ K}$.

growth of these linear defects, which can in turn be understood through the higher temperature at which the Bi-2223 phase forms.

B. Reversible magnetic properties

Figure 5 shows the reversible magnetization M of Bi-25-UD as function of temperature near T_c in different fields. Within experimental error, all the $M(T)$ curves intersect at the same crossing point (M^*, T^*) , with $T^* = 64.6 \text{ K}$. The crossing point is the result of the 2D nature of the critical fluctuations in the strongly layered superconductors. We thus use 2D scaling for the magnetization at temperature T for various fields H not far away from H_{c2} .^{11,19,20} The inset to Fig. 5 shows M/\sqrt{TH} plotted against the scaling parameter $[T - T_c(H)]/\sqrt{TH}$ for fields above 0.5 T. It is seen that our data follow the 2D scaling very well if we take $T_c(H) = T_c(0) - H/H'_{c2}$ with $\mu_0 H'_{c2} = \mu_0 (\partial H_{c2} / \partial T)_{T=T_c} = 0.82 \text{ T/K}$ and $T_c(0) = T_{c0} = 69.6 \text{ K}$ ($\mu_0 = 4\pi \times 10^{-7} \text{ Hm}^{-1}$). Furthermore, we could determine the Ginzburg-Landau coherence length $\xi(0)$ from the relation $\mu_0 H'_{c2} = \Phi_0 / 2\pi \xi(0)^2 T_c(0)$ and obtained $\xi(0) = 2.5 \text{ nm}$. The same analysis for Bi-25-OP and Bi-25-OV yields the results in Table II. It is seen that T_{c0} is significantly higher than the true T_c determined from the ac susceptibility, suggesting that the temperature range between T_{c0} and T^* should be identified as the critical fluctuation regime.²² This regime decreases for the optimally doped and overdoped samples.

The measurement of the reversible magnetization is often used to determine the value of the penetration depth $\lambda(T)$ and the superfluid density n_s . In the mean-field London approximation the reversible magnetization is given by

$$M_0 = -\frac{\epsilon_0}{2\Phi_0} \ln\left(\frac{\eta H_{c2}}{H}\right). \quad (1)$$

TABLE II. Properties of post-annealed Bi-2212 single crystals grown in $P_{O_2}=25$ mbar.

Samples	T_c (K)	δT_c (K)	c (nm)	T^* (K)	T_{c0} (K)	H'_{c2} (T/K)	$\xi(0)$ (nm)
Bi-25-UD	65.0	2.5	3.090	64.4	69.6	0.82	2.5
Bi-25-OP	87.3	1.0	3.086	86.1	90.1	2.0	1.3
Bi-25-OV	77.0	1.0	3.080	76.6	78.4	1.2	1.8

Here $\varepsilon_0(T) = \Phi_0^2/[4\pi\mu_0\lambda^2(T)]$ and $\eta \sim 0.35$ is a constant of order unity. In layered quasi-2D superconductors thermally driven positional fluctuations of the pancake vortices were suggested to give rise to an entropic term M_1 which should be added to the reversible magnetization near T_c .^{11,19} The entropy term for single pancake vortices is given by

$$M_1 = \frac{k_B T}{s\Phi_0} \ln\left(\frac{H_0}{H}\right), \quad (2)$$

where $s \approx 15.4$ Å is the interlayer distance for Bi-2212 and H_0 is a characteristic field of order H_{c2} determined by the Gaussian excitations of the order parameter in the vortex core.²² Obviously, the total magnetization $M = M_0 + M_1$ should also be proportional to $\ln H$, but the temperature dependence of the slope should differ from the $\lambda^{-2}(T)$ behavior. This has been observed by, e.g., Li *et al.*²³ and van der Beek *et al.*²⁴

Figure 6 shows the reversible magnetization M of Bi-25-UD as function of field H at different temperatures. The absolute values of M decrease more or less proportionally to $\ln(1/H)$. In Fig. 7 we plot the measured $dM/d(\ln H)$ (open circles) determined from the logarithmic slopes of M above $\mu_0 H = 0.3$ T in Fig. 6. To demonstrate the possible effect of an entropy term (2) we also plot $d(M - M_1)/d(\ln H)$ vs T (open diamonds). Obviously, the term $dM_1/d(\ln H) = k_B T/(s\Phi_0)$ is much larger than $dM/d(\ln H)$ in a wide range of temperatures. If we linearly extrapolate $d(M - M_1)/d(\ln H)$ to zero (see the dotted line in Fig. 7), the

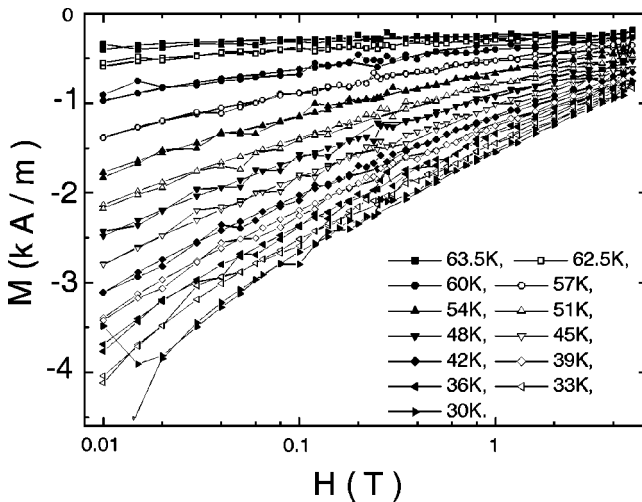


FIG. 6. Field dependence of magnetization of the Bi-25-UD, measured from 30 K to 63.5 K. The reversible magnetization was determined from the supposed measurements increasing and decreasing field.

intersection occurs at 84 K, nearly 14 K higher than the measured mean-field critical temperature T_{c0} (determined from the scaling analysis) to which we expect this line should extrapolate. Therefore it seems that the term M_1 overestimates the entropy contribution.

Recently van der Beek *et al.*²¹ introduced a phenomenological parameter K as a measure for the correlation length L_a over which pancake vortices are aligned along the c axis: $L_a = Ks$. Pancake correlations reduce the entropy term by a factor K . In principle, K could depend on temperature, but for the transparency of the analysis we choose K to be constant. Determining $\lambda^2(0)/\lambda^2(T)$ for optimally doped Bi-2212 from $M_0 = M - M_1/K$ with $K=3$, Rykov and Tamegai obtained good agreement with the penetration depth values which resulted from surface impedance measurements.²⁵

Pursuing this line of thought we assume that the mean-field magnetization near T_c can be written as $M = M_0 + M_1/K$; outside the critical regime, the open squares in Fig. 7 are described by

$$\frac{dM}{d(\ln H)} = \frac{\varepsilon_0(T)}{2\phi_0} - \frac{k_B T}{Ks\phi_0}, \quad (3)$$

with $\varepsilon_0(T) = \varepsilon_0(0)(1 - T/T_{c0})$ and $\varepsilon_0(0) = \Phi_0^2/[4\pi\mu_0\lambda_{GL}^2(0)]$, where $\lambda_{GL}(0)$ is the Ginzburg-Landau penetration depth at $T=0$ K. At T^* the magnetization is independent of field, i.e., $dM/d(\ln H) = 0$, which means that at T^* we have

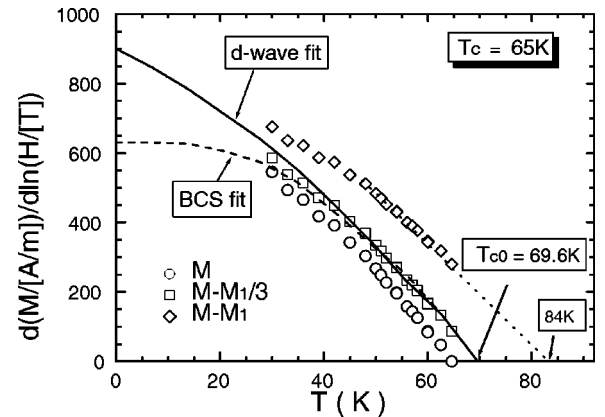


FIG. 7. Temperature dependence of logarithmic slopes $dM/d \ln H$, with M the measured magnetization (\circ), the modified correction $M - M_1/3$ (\square) and $M - M_1$ (\diamond) for the sample Bi-25-UD. The solid and dashed lines are fitting by the BCS and d -wave theory, respectively. The two fitting methods give the values of $\lambda_{BCS}(0) = 323$ nm and $\lambda_{d-wave}(0) = 269$ nm. The dotted line near T_c shows the large entropy term $M_1(T)$ compared to $M(T)$.

TABLE III. The fitting results of the different doped Bi-25 samples. All units of λ are in nm.

Samples	K	$\lambda_{GL}(0)$	$\lambda_L(0)$	$\lambda_{d-wave}(0)$	$\lambda_{BCS}(0)$
Bi-25-UD	3.2	235	322	269	323
Bi-25-OP	3.5	163	230	185	213
Bi-25-OV	4.8	136	192	168	196

$$\frac{\varepsilon(T^*)}{2\phi_0} = \frac{k_B T^*}{Ks\phi_0}. \quad (4)$$

The derivative $\partial^2 M / \partial T \partial \ln H$ obeys the relation

$$-\frac{d}{dT} \left(\frac{dM}{d(\ln H)} \right) = \frac{\varepsilon_0(0)}{2\phi_0 T_{c0}} + \frac{k_B}{Ks\phi_0}, \quad (5)$$

which is nearly independent of T . Using Eq. (4) this can also be written as

$$-T^* \frac{d}{dT} \left(\frac{dM}{d(\ln H)} \right) = \frac{\phi_0}{8\pi\mu_0\lambda_{GL}^2(0)}. \quad (6)$$

It is remarkable that this relation, from which $\lambda_{GL}(0)$ can be obtained, does not contain T_{c0} or K . We see that the effect of the entropy term in comparison to the simple mean-field approach is a replacement of T_{c0} by T^* in Eq. (6). Therefore the error in $\lambda_{GL}(0)$ by not accounting for the entropy term in previous analyses is not very big, only 1%–2% as follows from Table II. The values of $\lambda_{GL}(0)$ and the London penetration depth $\lambda_L(0) = \sqrt{2}\lambda_{GL}(0)$ which were obtained this way are summarized in Table III for these Bi-25 samples. The results compare satisfactorily with previous results.⁵ Once $\lambda_{GL}(0)$ is determined, the value of the parameter K immediately follows from Eq. (4). For Bi-25-UD we got $K = 3.2$, whereas $K = 3.5$ and $K = 4.8$ resulted for the optimally doped and overdoped samples. Physically we should expect integer numbers for K . The noninteger value for K , e.g., $K = 3.2$, may be interpreted as the average of correlated stacks of mostly three pancake vortices and sometimes more and sometimes less.

It is quite surprising that in the liquid regime of Bi-2212 for several doping levels the pancake vortices are still somehow correlated in the c direction and not completely decoupled. We note that there exists a relation between the values of K in Table III and the anisotropy which decreases with oxygen doping. The same conclusion has been arrived by Rykov and Tamegai.²⁵ We also point out that when we plot $d(M - M_1/K)/d(\ln H)$ vs T (the squares in Fig. 7) with $K = 3$, the intersection with the T axis occurs at 69.5 K, which coincides well with the value for T_{c0} that was determined from the 2D scaling analysis in the critical regime. The squares in Fig. 7 thus represent a corrected data set from which the temperature dependence of the penetration depth can be deduced.

The mean-field behavior of $\lambda^2(0)/\lambda^2(T)$ should follow the $dM_0/d(\ln H)$ data and provide $\lambda(0)$ as a fitting parameter. The London penetration depth for s -wave superconduct-

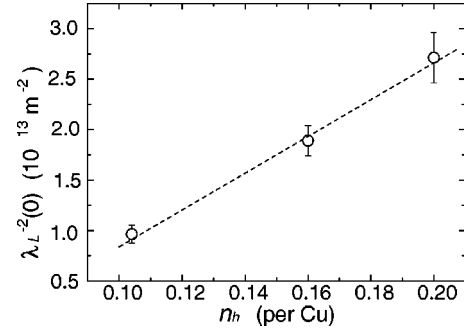


FIG. 8. $1/\lambda_L^2(0)$ vs hole number per Cu, n_h , for Bi-25-UD to Bi-25-OP and Bi-25-OV, from left to right, respectively. The dashed line is a guide to the eyes.

ors should follow from a pure limit BCS fit,¹⁰ given by the dashed line in Fig. 7, yielding $\lambda_{BCS}(0) = 323$ nm. Within experimental error this is indeed the case (see Table III), which supports the validity of the correction procedure for the entropy term. The drawn line in Fig. 7 displays the temperature dependence for a d -wave superconductor⁹ with fit parameter $\lambda_{d-wave}(0) = 269$ nm. The values for the other samples are given in Table III. Below 30 K a comparison between theoretical fits is made impossible because of flux pinning. This is unfortunate, because the clean-limit BCS fit is doing just as well as the d -wave fit. It is also seen that the average d -wave penetration depth at zero temperature is appreciably smaller than the London result.

Finally, we show in Fig. 8 how for our Bi-25 samples the zero-temperature penetration depth depends on the hole number per Cu, n_h , by plotting $1/\lambda_L^2(0)$ versus n_h . The latter was determined by using the empirical relation given by Presland *et al.*²⁶: namely, $T_c/T_c^{max} = 1 - 82.6(n_h - 0.16)^2$, where for the cation composition of samples $T_c^{max} \approx 87.3$ K.²⁷ Within the error bars we find a linear dependence over the entire doping regime from strongly underdoped to moderately overdoped.

IV. CONCLUSIONS

In conclusion, we showed that the doping levels of as-grown Bi-2212 crystals are very sensitive to the partial pressure of oxygen during growth. Interestingly, Bi-2212 single crystals grown in $P_{O_2} = 25$ mbar are excellent for further research because of high quality and the possibility to vary the doping levels from strongly underdoped to slightly overdoped by means of post-anneal treatments. By analyzing the reversible magnetization of the strongly underdoped sample within the existing theoretical models we obtained some superconducting parameters, such as its penetration depth $\lambda(T)$ and coherence length $\xi(0)$. We found that the effect of the thermal fluctuations was not as large as expected for entirely decoupled pancake vortices. Correlated stacks of three to five pancakes could explain the data well. The temperature dependence of the corrected empirical $dM/d(\ln H)$ could be fitted equally well by both the d -wave pairing and the BCS clean-limit theory.

ACKNOWLEDGMENTS

We would like to acknowledge the assistance of T. J. Gortenmulder and R. W. A. Hendriks for EPMA and x-ray analysis. We are grateful to the Europe Scientific Foundation (ESF) and the Netherlands Organization for Scientific Re-

search (NWO) for financial support. This work is part of the research program of the Amsterdam-Leiden material research cooperation (FOM-ALMOS) supported by the Foundation for Fundamental Research on Matter (FOM) of the Netherlands.

-
- ¹G. Villard, D. Pelloquin, and A. Maignan, *Phys. Rev. B* **58**, 15 231 (1998).
- ²B. vomHedt, W. Lisseck, K. Westerholt, and H. Bach, *Phys. Rev. B* **49**, 9898 (1994).
- ³T. Motohashi, Y. Nakayama, T. Fujita, K. Kitazawa, J. Shimoyama, and K. Kishio, *Phys. Rev. B* **59**, 14 080 (1999).
- ⁴H. Ding *et al.*, *Nature (London)* **382**, 51 (1996).
- ⁵T. W. Li, P. H. Kes, N. T. Hien, J. J. M. Franse, and A. A. Menovsky, *J. Cryst. Growth* **135**, 481 (1994); T. W. Li *et al.*, *Physica C* **257**, 179 (1996).
- ⁶A. Q. Pham *et al.*, *Physica C* **194**, 243 (1992).
- ⁷K. Kishio, J. Shimoyama, Y. Kotaka, and K. Yamafuji, in *Proceedings of the 7th International Workshop on Critical Current in Superconductors*, edited by Harald W. Weber (World Scientific, Singapore, 1994), p. 339.
- ⁸T. Watanabe, T. Fujii, and A. Matsuda, *Phys. Rev. Lett.* **79**, 2113 (1997).
- ⁹R. J. Radtke, V. N. Kostur, and K. Levin, *Phys. Rev. B* **53**, R522 (1996).
- ¹⁰B. MÜCHLSCHLEGEL, *Z. Phys.* **155**, 313 (1959).
- ¹¹Dingping Li and Baruch Rosenstein, *Phys. Rev. Lett.* **86**, 3618 (2000).
- ¹²N. Motohira, K. Kuwahara, T. Hasegawa, K. Kishio, and K. Kitazawa, *J. Ceram. Soc. Jpn.* **97**, 994 (1989).
- ¹³L. A. Dorosinskii, M. V. Indenbom, V. I. Nikitenko, Yu. A. Ossip'yan, A. A. Polyanskii, and V. K. Vlasko-Vlasov, *Physica C* **203**, 149 (1992).
- ¹⁴Xin-Fen Chen, G. X. Tessema, and M. J. Skove, *Physica C* **181**, 340 (1991).
- ¹⁵Y. Tajima, M. Hikita, M. Suzuki, and Y. Hidaka, *Physica C* **158**, 237 (1989).
- ¹⁶Arif Mumtaz, Yuli Yamaguchi, Kunihiko Oka, and Guruswamy Rajaram, *Physica C* **302**, 331 (1998).
- ¹⁷N. Chikumoto, E. Yasuda, and M. Murakami (unpublished).
- ¹⁸R. J. Drost, Ph.D thesis, Leiden University, 1999.
- ¹⁹L. N. Bulaevskii, M. Ledvij, and V. G. Kogan, *Phys. Rev. Lett.* **68**, 3773 (1992).
- ²⁰B. Rosenstein, B. Ya. Shapiro, R. Prozorov, A. Shaulov, and Y. Yeshurun, *Phys. Rev. B* **63**, 134501 (2001).
- ²¹C. J. van der Beek, M. Konczykowski, R. J. Drost, P. H. Kes, N. Chikumoto, and S. Bouffard, *Phys. Rev. B* **61**, 4259 (2000).
- ²²A. E. Koshelev, *Phys. Rev. B* **50**, 506 (1994).
- ²³Q. Li, K. Shibusaki, M. Suenaga, I. Shigaki, and R. Ogawa, *Phys. Rev. B* **48**, 9877 (1993).
- ²⁴C. J. van der Beek, M. Konczykowski, T. W. Li, P. H. Kes, and W. Benoit, *Phys. Rev. B* **54**, R792 (1996).
- ²⁵Alexandre I. Rykov and Tsuyoshi Tamegai, *Phys. Rev. B* **63**, 104519 (2001).
- ²⁶M. R. Presland, J. L. Tallon, R. G. Buckley, R. S. Liu, and N. E. Flower, *Physica C* **176**, 95 (1991).
- ²⁷By fine-tuning the oxygen content we determined the highest T_c values; for Bi-25 crystals, this was $T_c^{max}=87.3$ K, and for the Bi-200 crystals, it was $T_c^{max}=90.5$ K.